Journal of Medicinal Chemistry Article

J. Med. Chem. **2011,** *54,* 277–283 **277**
DOI: 10.1021/jm101156y

Pipecolic Acid Derivatives As Small-Molecule Inhibitors of the *Legionella* MIP Protein

Christina Juli,[†] Martin Sippel,[†] Jens Jäger,[‡] Alexandra Thiele,[§] Matthias Weiwad,[§] Kristian Schweimer,[∥] Paul Rösch,[∥] Michael Steinert,[‡] Christoph A. Sotriffer,[†] and Ulrike Holzgrabe*[,†]

[†]*Institute of Pharmacy and Food Chemistry, University of Würzburg, Am Hubland, 97074 Würzburg, Germany,* [‡]*Institut für Mikrobiologie, Technische Universität Braunschweig, Spielmannstrasse 7, 38106 Braunschweig, Germany,* [§]*Research Center for Enzymology of Proteinfolding, Max-Planck-Institute Halle, Weinbergweg 22, 06120 Halle, Germany, and* [∥]*Department of Biopolymers, University of Bayreuth, Universitätsstrasse 30, 95447 Bayreuth, Germany*

Received September 7, 2010

The macrophage infectivity potentiator (MIP) protein is a major virulence factor of *Legionella pneumophila*, the causative agent of Legionnaires' disease. MIP belongs to the FK506-binding proteins (FKBP) and is necessary for optimal intracellular survival and lung tissue dissemination of *L. pneumophila*. We aimed to identify new small-molecule inhibitors of MIP by starting from known FKBP12 ligands. Computational analysis, synthesis, and biological testing of pipecolic acid derivatives revealed a promising scaffold for new MIP inhibitors.

Introduction

Legionella pneumophila is a Gram-negative aerobic pathogen causing two distinct forms of Legionellosis: Legionnaires' disease, a severe form of pneumonia with a mortality rate of up to 20%, and Pontiac fever, a milder respiratory disease with symptoms resembling acute influenza.[1] The pathogen naturally inhabits fresh waters and biofilms, where it parasitizes within protozoan hosts. Human infection is by inhaling aerosols from contaminated man-made hot water systems. Elderly adults, smokers, and people with impaired immunity are particularly susceptible. The pathogen can colonize the lung and replicate intracellularly within macrophages. During the replicative phase the bacteria reside within a maturation blocked phagosome. Infection studies in different host cell models revealed that the *Legionella* virulence factor MIP protein contributes to the establishment of infection.[2,3] Guinea pig infections with MIP-positive and MIP-negative *L. pneumophila* strains and mutants showed that MIP also contributes to bacterial dissemination within the lung. Binding assays with components of the extracellular matrix (ECM[a]) demonstrated the interaction of MIP with collagen IV, the prevalent collagen in the human lung.[4] Degradation assays with ECM proteins supported the hypothesis of a concerted action of MIP and other proteolytic enzyme activities, although the exact role of MIP in this process remains to be established.[4−6]

The MIP protein is a peptidyl prolyl *cis*/*trans* isomerase (PPIase) belonging to the FK506 binding protein family. It forms an extremely stable complex with the immunosuppressive drugs FK506 and rapamycin which both inhibit the enzymatic function of MIP.[6] However, these drugs are contraindicated for treatment of Legionnaires' disease because they interact with human FKBPs exerting immunosuppressive effects. Recently, Ceymann et al. solved the structure of free MIP protein and the MIP−rapamycin complex by means of nuclear magnetic resonance (NMR) spectroscopy.[7] The complex structure revealed that binding to MIP is mainly mediated by rapamycin's pipecoline moiety, which is anchored in a hydrophobic pocket of the binding site. This is similar to FKBP12 (a human PPIase playing a crucial role in immunological processes), which lends credence to the hypothesis that non-immunosuppressive small-molecule inhibitors of FKBP12 derived from rapamycin, may constitute a suitable starting point for obtaining low-molecular-weight inhibitors of the MIP protein. Accordingly, the goal of this work is the development of pipecolic acid derivatives as MIP inhibitors by a combined approach of structure comparison, computational analysis, chemical synthesis, and experimental testing, including enzymatic methods, cell-based measurements, and NMR HSQC experiments.

Results and Discussion

MIP is a homodimeric protein consisting of two 22.8 kDa monomers. Homodimerization is mediated by the N-terminal domain, which is connected through a long helix to the C-terminal domain that resembles FKBP12 and contains the rapamycin binding site. This C-terminal or FKBP domain extends from residues 77 to 213 (MIP^{77-213}) of the full-length protein. In all of the following, "MIP" refers only to this domain (with the residues numbered consecutively from 1 to 137). Currently, three MIP structures are available in the PDB: A crystal structure (1FD9)[8] and an NMR solution structure (2UZ5)[7] of the unbound protein, as well as an NMR structure with rapamycin bound to the active site (2VCD).[7] The structures reveal a domain consisting of six β-strands which

*To whom correspondence should be addressed. Phone: +49-931-3185460. Fax: +49-931-3185494. E-mail: u.holzgrabe@pharmazie.uni-wuerzburg.de.

[a]Abbreviations: MIP, macrophage infectivity potentiator; FKBP, FK506 binding protein; ECM, extracellular matrix; HSQC, heteronuclear single quantum coherence; PDB, protein database; rmsd, root-mean-square deviation; cf., confer; DCC, dicyclohexylcarbodiimide; DMAP, dimethylaminopyridine; PPIase, peptidyl prolyl isomerase; GA, genetic algorithm; TLC, thin layer chromatography; FT-IR, Fourier transform infrared spectroscopy; HEPES, 2-(4-(2-hydroxyethyl)-1-piperazinyl)-ethanesulfonic acid.

Published on Web 12/13/2010

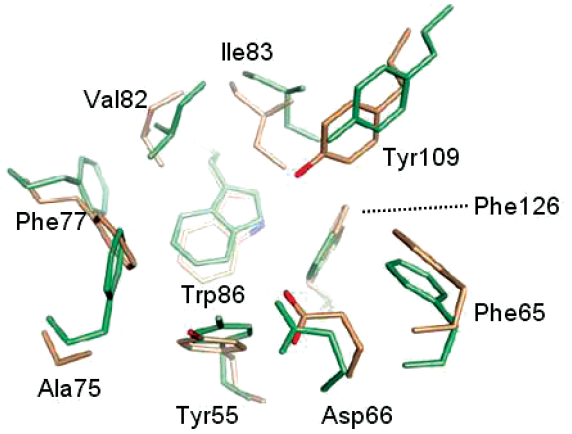

Figure 1. Comparison of the binding pockets of MIP (colored wheat, with residue numbers) and FKBP12 (colored green) in the rapamycin complexes (MIP, 2VCD; FKBP12, 1FKB). In MIP, Tyr109 (top right) protrudes deeper into the pocket.

form an antiparallel sheet and a short helix positioned across this sheet. The active site is located right between this helix and the internal side of the sheet and shows a predominantly hydrophobic character. It is formed by Tyr55, Ala75, Phe77, Val82, Ile83, and Phe126, as well as Trp86 at the ground of the pocket. Phe65, Asp66, and Tyr109 are located at the outer rim of the pocket and are responsible for the main conformational differences among the three available structures. Because of the higher relevance of complex structures for the ligand-bound state of a protein, only structure 2VCD was used for all subsequent analyses.

Comparison of MIP with FKBP12 reveals highly homologous binding sites formed by identical amino acids, except for Ala75, which corresponds to a phenylalanine residue in FKPB12. Nevertheless, superposition of the rapamycin complexes of MIP and FKBP12 (PDB 1FKB) shows significant differences, in particular with respect to Tyr109, which protrudes much deeper into the binding pocket of MIP, thereby reducing its overall size (Figure 1). This is reflected by differences in the binding mode of the pipecoline moiety of rapamycin with respect to the orientation of the aliphatic ring in the hydrophobic pocket, the conformation of the ester, and the hydrogen-bonding pattern of the carbonyl groups. This leads to the expectation that also the binding of small molecules may show differences among the two proteins.

Various FKBP12 ligands have been described in the literature. Among them are compounds which bear a pipecoline moiety, thus resembling the rapamycin anchoring group. However, these ligands lack the macrocyclic portion of rapamycin, thereby abolishing the immunosuppressive action. Given the known binding of rapamycin to MIP, these compounds should constitute the best starting point for obtaining new MIP inhibitors. Accordingly, the two submicromolar FKBP12 inhibitors **A** ($K_i = 0.010\,\mu M$)[9] and **B** ($K_i = 0.230\,\mu M$)[10] were selected for investigation (Figure 2).

For **A**, a crystal structure in complex with FKBP12 is available (PDB 1FKG), showing an analogous binding mode as the pipecoline group of rapamycin. As a reference, ligand **A** was separated from the protein and computational redocking was carried out to reconstitute the complex. This reproduced the experimental binding mode as top-ranked, well-clustered result with a root-mean-square deviation (rmsd) of 1.05 Å. Docking of **A** to MIP with the same procedure yielded a top-ranked binding mode which also placed the pipecoline ring in

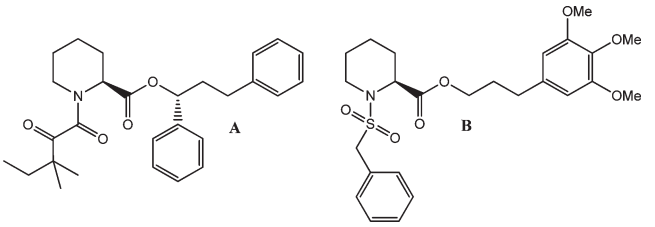

Figure 2. FKBP12 inhibitors selected for investigation.

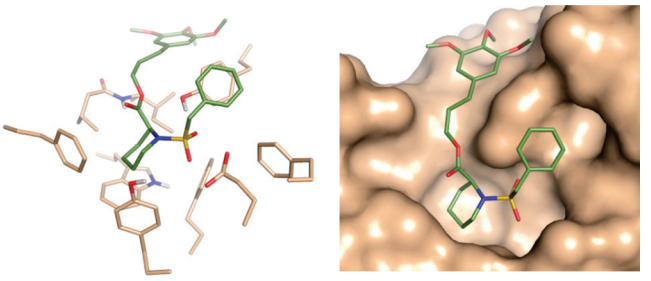

Figure 3. Top-ranked binding mode of **B** (corresponding to ***S*-4c**, cf. below) in MIP. The pipecoline ring is placed in the active-site pocket, showing good shape complementarity.

the active-site pocket. However, although similarities in the orientation exist, the placement does not overlap very well with the rapamycin binding mode in MIP. Furthermore, this result was obtained only in 2 out of 100 runs, whereas another orientation (which placed the phenyl ring in the hydrophobic pocket) was obtained more frequently. More importantly, the docking score for **A** in MIP was significantly less favorable than the top-ranked score of **A** in FKBP12. Taken together, these results suggest that although binding of **A** to MIP may be possible, it is unlikely to result in a perfectly matching binding mode leading to high affinity.

Subsequently, docking to MIP was carried out with compound **B**, for which no crystal structure with FKBP12 is available. This time, a well-clustered top-ranked result was obtained, showing a very favorable hydrophobic interaction score, which was even better than the score obtained upon docking of **B** to FKBP12. Indeed, the binding mode of **B** in MIP shows a good fit of the pipecoline-sulfonamide anchor group, which is reflected in the high hydrophobic score (Figure 3). In contrast to the α-ketoamide moiety of **A**, the less bulky sulfonamide of **B** allows for a better placement in the narrow MIP pocket. These observations refer to the *S*-enantiomer of the ligand (as shown in Figure 3). The *R*-enantiomer can also be placed in the pocket, but only in a somewhat distorted orientation, leading to a less favorable hydrophobic score.

Given these observations, compounds **A** and **B** (***S*-4c**) were approached by synthesis. Instead of compound **A**, a slightly modified analogue with an isobutyl chain instead of the 2,2-dimethylpropyl substituent was more readily accessible and, thus, synthesized initially. On the basis of the binding model, the modification was not expected to have any significant influence on the activity. On the other hand, the benzylsulfonamide **B** (***S*-4c**) was prepared, as well as the corresponding phenylsulfonamide (i.e., compound **4d** below). Docking showed a convincing binding mode similar to **B** (***S*-4c**) for this phenyl derivative, although with a significantly less favorable hydrophobic score but granting possibilities for aromatic substitution in *meta* position. Accordingly, meta-substituted derivatives of the phenylsulfonamide were synthesized as well.

Scheme 1. Synthetic Route to the Pipecolic Acid Derivatives[a]

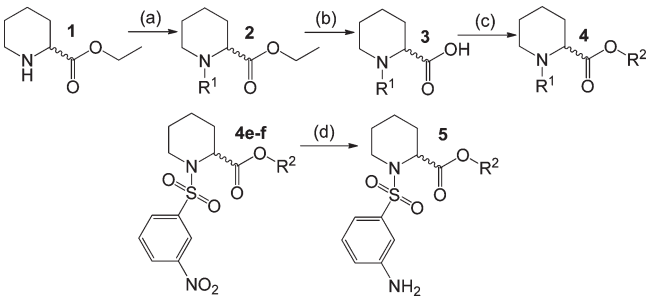

[a] Reagents and conditions, (a) R^1-Cl, NEt_3, DMF, RT, 6 h; (b) LiOH, MeOH, 0 °C, 1 h; (c) R^2-OH, DCC, DMAP, *p*-toluene sulfonic acid, CH_2Cl_2, RT, 72 h; (d) $SnCl_2$, EtOH, reflux, 2 h.

The general synthetic route is illustrated in Scheme 1. Synthesis of the pipecolic acid derivatives started with the conversion of commercially available ethyl piperidine-2-carboxylate hydrochloride with 3 equiv of triethylamine and equimolar amounts of sulfonyl or carbonyl chloride, leading to the amides **2a**−**d**. Subsequently, the ethyl ester was hydrolyzed using lithium hydroxide to give the free pipecolic acids **3a**−**d**. To obtain the corresponding esters **4a**−**f**, the free acids were converted with equimolar amounts of the corresponding alcohols, 1.5 equiv of dicyclohexylcarbodiimide, catalytic amounts of dimethylaminopyridine, and *p*-toluene sulfonic acid. The enantiopure compound **B** (***S*-4c**) was synthesized by employing the enantiopure pipecolic acid as starting material. The nitro analogues (**4e** and **4f**) were reduced via $SnCl_2$ to the corresponding amino compounds **5a** and **5b**, respectively (see Scheme 1). The structures of all compounds were confirmed by NMR spectroscopy.

The inhibition of MIP was determined by a protease-coupled PPIase assay. This PPIase activity catalyzed by recombinant MIP expressed in *Escherichia coli* was determined using the synthetic peptide succinyl-Ala-Phe-Pro-Phe-4-nitroanilide as substrate in the chymotrypsin-coupled reaction as previously described.[11] Because some of the tested compounds resemble common FKBP12 inhibitors,[9] the inhibition of FKBP12 was additionally analyzed by the same method. Most of the compounds were found to inhibit FKBP12 but not necessarily the MIP protein. The anti-MIP and anti-FKBP activity of the compounds is depicted in Table 1. IC_{50} values > 100 μM for MIP and > 30 μM for FKBP12 were not determined. (Note that the IC_{50} values should only be compared within the inhibitor series of one enzyme, but not between the two enzymes).

With ethyl as R^2 substituent attached to the carboxy function, the compounds show only weak inhibition of MIP (**2b**) or no sufficient effect below 100 μM concentration (**2a**, **2c**−**d**). This indicates a larger ester moiety is required for proper binding. However, addition of larger R^2 substituents to the α-ketoamide **2a** (resulting in compounds **4a** and **4b**) did not lead to any observable gain in activity against MIP. This is in contrast to FKBP12, where addition of the propyl-trimethoxyphenyl substituent to **2a** provides a clear gain in potency (compound **4b**). Apparently, the dicarbonyl-alkyl group of **2a** (and **4a**, **4b**) is not well suited to fit the MIP binding pocket. The lack of activity (below 30 μM) of **4a** in FKBP12 despite the reported submicromolar K_i of **A**[9] should most likely not only be attributed to the missing methyl group in **4a** but rather to the fact that **4a** was obtained and tested as mixture of 8 stereoisomers. In contrast to **4a** and **4b**, compounds **4c**, **4d**, and **4e** show substantial activity against MIP. The racemic compound **4c** shows the lowest IC_{50} of this series, which indicates that a methylene group next to the sulfonamide is advantageous for binding, in agreement with the modeling data. In the case of FKBP, instead, the phenyl and benzyl sulfonamide derivatives showed equal activity, pointing to a further difference in comparison to MIP. The introduction of a nitro group (**4f**) is detrimental to the MIP activity when compared with **4d**. Some activity can be restored by replacing the trimethoxyphenyl group with a pyridyl substituent (**4e**). The reduction of the nitro group to the corresponding amines does not lead to active compounds against MIP. Because the racemic compound **4c** was identified as the most promising MIP inhibitor, the corresponding enantiopure compound **B** (***S*-4c**) was synthesized. As anticipated, the *S*-enantiomer shows higher activity against MIP (IC_{50} = 6 μM). Given this potency, it represents a promising starting structure for the development of further inhibitors.

To prove the binding to the MIP protein, the interaction of compounds **2b**, **4c**, and **B** (***S*-4c**) with MIP was determined by means of NMR-HSQC experiments. The activity of the

Table 1. Synthesized Pipecolic Acid Derivatives and Their IC_{50} Values

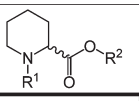

Entry	R^1	R^2	IC_{50} ± sdv [μM]; MIP	IC_{50} ± sdv [μM]; FKBP
2a	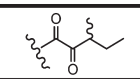		>100	>30
2b	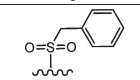		87 ± 5	2.6 ± 0.4
2c	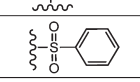		>100	3.1 ± 0.2
2d	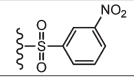		>100	2.8 ± 0.1
4a	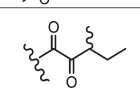	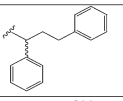	>100	>30
4b	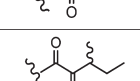	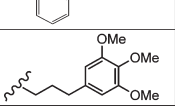	>100	4.2 ± 0.2
4c	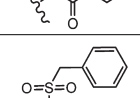	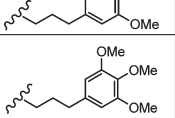	9 ± 0.7	0.2 ± 0.02
B (*S*-4c)	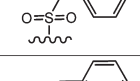		6 ± 0.7	0.2 ± 0.03
4d	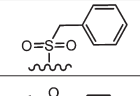	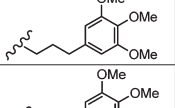	28 ± 1.7	0.12 ± 0.1
4e	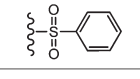	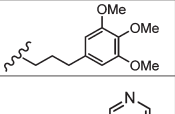	32 ± 2.4	0.15 ± 0.01
4f	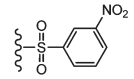	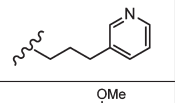	>100	0.07 ± 0.001
5a	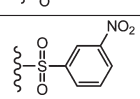	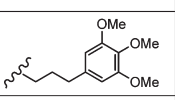	>100	0.32 ± 0.03
5b	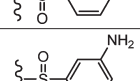	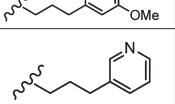	>100	0.26 ± 0.03

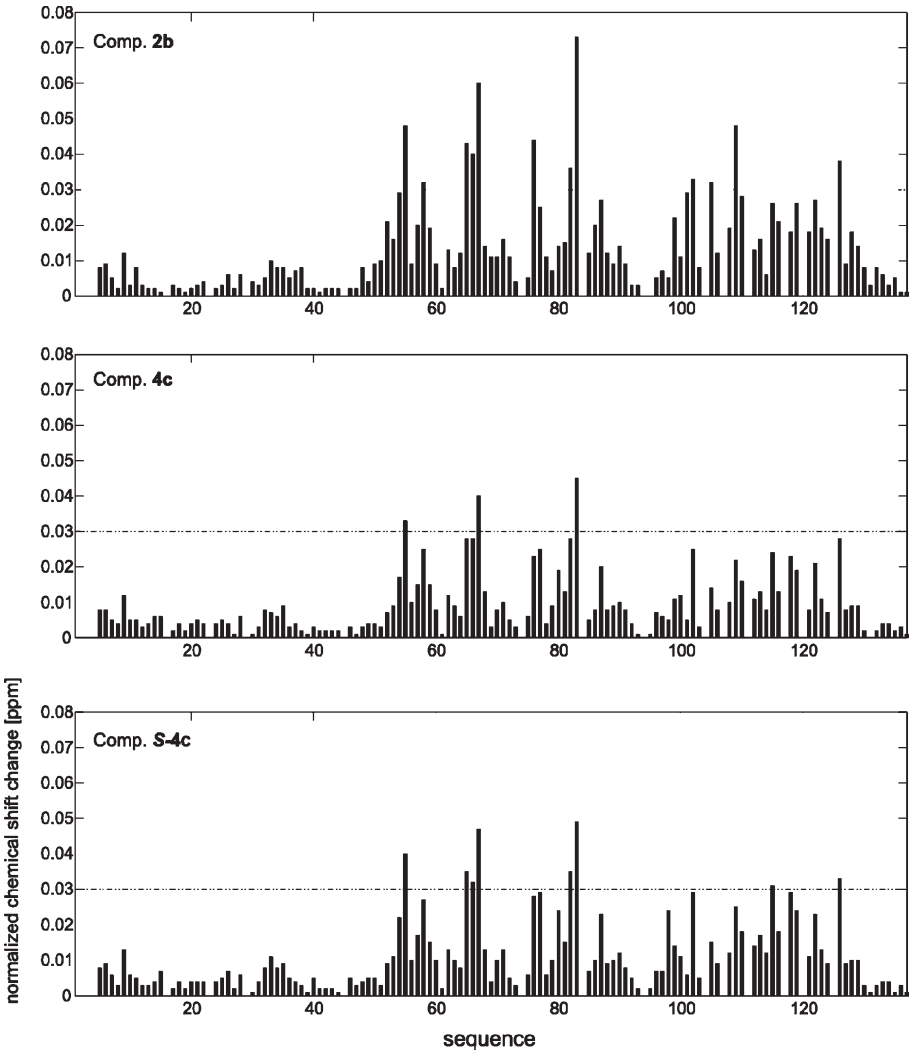

Figure 4. Changes in the chemical shifts of MIP residues as measured by NMR-HSQC experiments with compounds **2b**, **4c**, and **B** (***S*-4c**).

ligands was defined by changes in the chemical shifts. As can be seen in Figure 4, the titration of ^{15}N labeled MIP^{77-213} (FKBP domain) with compounds **2b**, **4c**, and **B** (***S*-4c**) resulted in significant chemical shift changes of several backbone amide resonances, indicating a strong binding of these compounds to the MIP-FKBP domain. Because of solubility problems at ligand:protein ratios of 20:1 (2 mM ligand, 0.1 mM protein), the saturation of MIP with the ligands could not be achieved; therefore, a determination of the dissociation constants was not possible.

The pattern of chemical shift changes is similar for all three ligands, indicating a similar binding mode at the same region of the protein. Mapping the chemical shift changes on the protein surface shows that the affected residues are located in the hydrophobic binding pocket for rapamycin. It is therefore concluded that the compounds **2b**, **4c**, and **B** (***S*-4c**) indeed bind to this cavity of MIP (see Figure 5).

To examine the influence of substance **B** (***S*-4c**) on invasion and intracellular replication, human macrophage-like U937-cells were infected with *L. pneumophila* Philadelphia-1 JR32 (wild type, WT), the MIP-negative mutant *L. pneumophila* JR32-2, and the *E. coli* strain HB101. The results of the gentamicin infection assays (Figure 6) revealed that substance **B** (***S*-4c**) does not influence the replication of wild type *L. pneumophila* JR32 in human macrophage-like U937 cells.

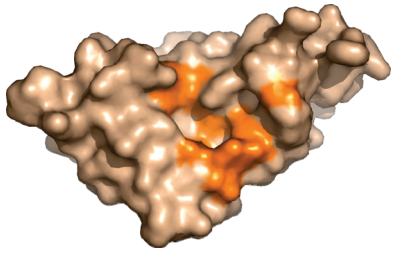

Figure 5. Structure of the MIP protein with binding regions (highlighted in orange) of compound **B** (***S*-4c**) as determined by NMR. The protein is seen from the same orientation as in Figure 3. The binding pocket is clearly recognizable in the center.

In contrast, rapamycin treated wild type *L. pneumophila* JR32, MIP-negative mutant *L. pneumophila* JR32-2 and *E. coli* strain HB101 were either not able to replicate in U937 cells or were degraded. These results confirm that the MIP protein, but not its PPIase activity, which is efficiently inhibited by substance **B** (***S*-4c**) (see Protease-Coupled PPIase Assay), is required for virulence on the cellular level of infection.[12] Moreover, these data support the hypothesis that the hydrophobic cavity of the PPIase domain rather confers bacterial adhesion to extracellular targets within lung tissue.[4] Thus, it will be interesting to identify the yet unknown target molecule

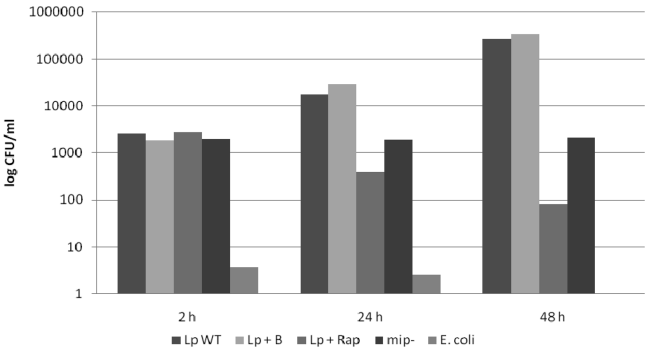

Figure 6. Influence of **B** (***S*-4c**) and rapamycin (Rap) on infection of U937 human macrophage-like cells. Lp = *Legionella pneumophila*, MIP− = MIP-deficient *L. pneumophila* strain.

of the MIP mediated PPIase activity and to analyze the effect of substance **B** (***S*-4c**) during guinea pig infections.

Experimental Section

Computational Docking. The MIP NMR structure 2VCD[7] was used for structural analyses and computational docking studies. Because 2VCD consists of an ensemble of 16 structures, the least restrictive conformation with respect to pocket size for ligand accommodation was selected. On the basis of the mutual distance between Asp66, Phe77, and Tyr109, 2VCD-4 (conformer 4) was used for this purpose. Focusing on the least restrictive conformation was based on the reasoning that upon docking at this exploratory stage, any ligand should be granted as much space as the protein is able to provide without any significant energy cost. Although this might not be the best conformation for all ligands, it should at least be the one which best prevents that true ligands are inadvertently excluded due to unsuccessful docking.

Docking was carried out with AutoDock3.0[13] and GOLD4.0.[14] For docking with AutoDock, the protein was setup by removing ligand and water molecules, as well as all hydrogen atoms. Polar hydrogens were then readded with the protonate tool, and Kollman united-atom partial charges and solvation parameters were assigned to all atoms.[15] The active site was defined by a box of $60 \times 60 \times 60$ grid points, centered between Phe77 and Tyr109. The grid spacing was set to 0.375 Å. Subsequently, the interaction maps were calculated with the autogrid module. Gasteiger−Marsili charges[16] were added to the ligand using Sybyl8.0.[17] The conversion to the pdbq format as well as the definition of rotatable bonds was done with the autotors module of AutoDock. The docking protocol used an initial population of 50 individuals, a maximum number of 3.0×10^6 energy evaluations, a mutation rate of 0.02, a crossover rate of 0.80, and an elitism value of 1. The Solis and Wets local search parameters were set as follows: The probability of performing a local search on an individual was set to 0.06, a maximum number of 300 iterations was performed, and the number of consecutive successes or failures before changing the size of the local search space was 4. 100 GA runs were carried out.

For docking with GOLD, the binding site was defined by a sphere of 8 Å radius, centered between Tyr55 and Tyr109 of the fully protonated 2VCD-4 structure. GOLDscore was used as scoring function. 50 GA runs were performed. Genetic algorithm parameters were set as follows: Population size 100, number of islands 5, selection pressure 1.1, number of operations 89500, niche size 2, migrate 10, mutate 95, and crossover 95.

Chemical Synthesis. ^{1}H and ^{13}C NMR spectra were recorded on an Avance 400 nuclear magnetic resonance spectrometer, Bruker Biospin GmbH, Rheinstetten, Germany (^{1}H 400.132 MHz, ^{13}C 100.613 MHz). As internal standard the signals of the deuterated solvents were used (DMSO-d_6: ^{1}H 2.50 ppm, ^{13}C 39.52 ppm, chloroform-*d*: ^{1}H 7.26 ppm, ^{13}C 77.16 ppm). The following abbreviations describing the multiplicity are used: (s) singlet, (d) doublet, (t) triplet, (q) quartet, (dd) doublet of doublet, (dt) doublet of triplet, (br) broad signal, (m) multiplet. Coupling constants are given in hertz. TLC was carried out on TLC aluminum sheets, silica gel F_{254} (Merck KGaA, Darmstadt, Germany). IR spectra were obtained with a Biorad PharmalyzIR FT-IR spectrometer (Biorad, Cambridge, MA, USA). Melting points were determined using a capillary melting point apparatus (Gallenkamp, Sanyo) and are uncorrected. The purity of the compounds was confirmed by quantitative microanalyses (C, H, N); the new compounds were in accordance with the theoretical value within ±0.4%, i.e., purity higher than 95%. All chemicals were purchased from Sigma-Aldrich Chemicals (Deisenhofen, Germany), Acros Organics (Geel, Belgium), and VWR International (Darmstadt, Germany) and were used without further purification. The peptide was purchased from Bachem Distribution Services GmbH (Weil am Rhein, Germany).

Below, the general synthesis procedures are reported, as well as experimental and spectroscopic details for the compounds ***S*-1**, ***S*-2b**, ***S*-3b**, and ***S*-4c**. Details for all other compounds can be found in the Supporting Information.

Synthesis of (*S*)-Ethyl piperidine-2-carboxylate *S*-1. (*S*)-Piperidine-2-carboxylic acid (1 equiv) was dissolved in 40 mL of anhydrous ethanol, and thionyl chloride (3 equiv) was added dropwise. The mixture was refluxed for 4 h under stirring. After the reaction had ceased (TLC control), the solvent was removed in vacuo. The residue was suspended in 20 mL of $NaHCO_3$ and washed with 4×30 mL $CHCl_3$. The organic layers were dried over anhydrous Na_2SO_4, and the solvent was removed in vacuo to yield compound (***S*)-1** as a yellow waxy substance (0.90 g, 90%). ^{1}H NMR ($CDCl_3$, δ [ppm], J [Hz]): 4.15 (q, 2H, ^3J = 7.1), 3.52 (dd, 1H, ^3J = 3.5, ^3J = 9.8), 3.22−3.14 (m, 1H); 2.79−2.69 (m, 1H), 2.03−1.95 (m, 1H), 1.92 (s, 1H), 1.77−1.40 (m, 5H), 1.22 (t, 3H, ^3J = 7.1). IR [cm^{-1}]: 1046, 1205, 1370, 1456, 1740, 2695, 2906.

General Procedure for the Synthesis of Compounds 2a−d and *S*-2b. Ethyl piperidine-2-carboxylate hydrochloride **1** and ***S*-1**, respectively (1 equiv), were dissolved in 40 mL of anhydrous DMF, and triethylamine (3 equiv) was added dropwise followed by carbonyl and sulfonyl chloride (1 equiv), respectively. The mixture was stirred for 6 h at RT and subsequently the solvent removed in vacuo. The residue was suspended in 30 mL $CHCl_3$ and washed with 4×30 mL 2 M HCl and H_2O. The organic layer was dried over anhydrous Na_2SO_4, and the solvent was removed in vacuo. If necessary, a subsequent purification by column chromatography was performed to obtain compounds **2a−d** and ***S*-2b.**

(*S*)-Ethyl 1-(Benzylsulfonyl)piperidine-2-carboxylate (*S*-2b). ***S*-2b** was obtained as a yellow oil (0.63 g; 70%). ^{1}H NMR ($CDCl_3$, δ [ppm], J [Hz]): 7.49−7.33 (m, 5H), 4.55−4.47 (m, 1H), 4.27 (s, 2H), 4.24−4.13 (m, 2H), 3.49−3.41 (m, 1H), 3.15 (dt, 1H, ^3J = 12.4, ^3J = 3.1), 2.20−2.12 (m, 1H), 1.73−1.52 (m, 3H), 1.51−1.37 (m, 1H), 1.33−1.20 (m, 4H). IR [cm^{-1}]: 1148, 1200, 1335, 1455, 1732, 2860, 2940. Anal. Calcd for $C_{15}H_{21}NO_4S$ (MW: 311.40 g/mol): C, 57.86; H, 6.80; N, 4.50; S, 10.30. Found: C, 58.17; H, 6.54; N, 4.78; S, 10.36.

General Procedure for the Synthesis of Compounds 3a−d and *S*-3b. The compounds **3a−d** and ***S*-3b**, respectively, were synthesized using a procedure described by Holt et al.[9] for analogous substances. Compounds **2** (1 equiv) were dissolved in 30 mL of methanol and cooled to 0 °C with an ice bath. To this mixture a solution of lithium hydroxide (10 mL, 1 M) was added dropwise, and then it was stirred for 1 h. After the reaction had ceased (TLC control), 10% HCl was added to adopt a pH value of 1. The free carboxylic acid was extracted with 4×30 mL CH_2Cl_2. The combined organic layers were washed with 4×50 mL H_2O and saturated NaCl and then dried over anhydrous Na_2SO_4. The solvent was removed in vacuo to give compounds **3a−d** and ***S*-3b**.

(*S*)-1-(Benzylsulfonyl)piperidine-2-carboxylic Acid (*S*-3b).[18] ***S*-3b** was obtained as a yellow oil (0.57 g, 90%). ^{1}H NMR ($CDCl_3$, δ [ppm], J [Hz]): 7.49−7.33 (m, 5H), 4.60−4.55 (m, 1H), 4.27 (s, 2H), 3.49−3.41 (m, 1H), 3.15 (dt, 1H, ^3J = 12.4, ^3J = 3.1); 2.20−2.12 (m, 1H), 1.73−1.52 (m, 3H), 1.51−1.18 (m, 2H). IR [cm^{-1}]: 1060, 1118, 1317, 1455, 1728, 2854, 2952, 3192.

General Procedure for the Synthesis of Compounds 4a−f and *S*-4c. The syntheses of compounds **4a−f** and ***S*-4c** were performed using a procedure described by Holt et al.[9] for analogous substances. Compounds **3** (1 equiv), the corresponding alcohol (1.1 equiv), DCC (1.5 equiv), DMAP (0.3 equiv), and *p*-toluene sulfonic acid (0.3 equiv) were dissolved in 50 mL of anhydrous CH_2Cl_2. This mixture was stirred for 72 h at RT. After the reaction had ceased (TLC control), the precipitate was filtered off and the solvent was removed in vacuo. The residue was suspended in ethyl acetate, and the resulting precipitate was filtered off again. This procedure was repeated as long as a precipitate was formed. Afterward, the filtrate was dried over Na_2SO_4 and subsequently the solvent removed in vacuo. If it was necessary, a subsequent purification by silica gel column chromatography was performed to obtain the compounds **4a−f** and ***S*-4c**.

(*S*)-3-(3,4,5-Trimethoxyphenyl)propyl 1-(benzylsulfonyl)-piperidine-2-carboxylate (*S*-4c). After purification by column chromatography (aluminum oxide; chloroform: ethyl acetate = 1:1) ***S*-4c** was obtained as a yellow waxy substance (0.12 g, 21%). ^{1}H NMR ($CDCl_3$, δ [ppm], J [Hz]): 7.49−7.33 (m, 5H), 6.41 (s, 2H), 4.55−4.50 (m, 1H), 4.27 (s, 2H), 4.24−4.15 (m, 2H), 3.84 (s, 6H), 3.82 (s, 3H), 3.46−3.40 (m, 1H), 3.17 (dt, 1H, ^3J = 12.4, ^3J = 3.1), 2.68−2.62 (m, 2H), 2.20−2.12 (m, 1H), 2.03−1.95 (m, 2H), 1.75−1.50 (m, 3H), 1.51−1.18 (m, 2H). IR [cm^{-1}]: 1124, 1335, 1455, 1589, 1733, 2857, 2938. Anal. Calcd for $C_{25}H_{33}NO_7S$ (MW: 491.60 g/mol): C, 61.08; H, 6.77; N, 2.85; S, 6.52. Found: C, 60.86; H, 6.87; N, 3.06; S, 6.13.

General Procedure for the Synthesis of Compounds 5a−b. The reduction of **4e** and **4f** was performed according to Bellamy et al.[19] Compound **4e** and **4f** (1 equiv), respectively, was suspended in 50 mL of anhydrous ethanol and $SnCl_2$ (5 equiv) added in portions. This reaction was refluxed for 2 h. The reaction was monitored by TLC (silica gel; triethylamine:ethylacetate = 5:95). Thirty mL of water and $NaHCO_3$ were added to neutralize the mixture. The aqueous phase was washed with 4 × 30 mL ethyl acetate. The combined organic layers were dried over anhydrous Na_2SO_4, and the solvent was removed in vacuo. If necessary, a subsequent purification by silica gel column chromatography was performed to obtain compounds **5a−b**.

Protease-Coupled PPIase Assay. The PPIase activity of MIP (and FKBP12, respectively) was determined by using the peptide substrate Succinyl-Ala-Phe-Pro-Phe-4-nitroanilide in the protease-coupled PPIase assay as described by Fischer et al.[6] To study the effect of compounds **2a−d**, **4a−f**, ***S*-4c**, and **5a−b** on PPIase activity, 40 nM MIP (20 nM FKBP12), and 40 μM peptide substrate were preincubated in the presence or absence of various inhibitor concentrations for 4 min at 10 °C in 35 mM HEPES/NaOH buffer (pH 7.8). Then reaction was started by addition of 100 μg/mL of the isomer specific protease chymotrypsin, and the release of 4-nitroaniline was monitored by measuring the absorbance at 390 nm.

NMR Spectroscopy: HSQC Experiments. ^{15}N labeled MIP^{77-213} was expressed and purified as described previously.[7] NMR samples contained 0.1 mM ^{15}N labeled MIP^{77-213} in 20 mM potassium phosphate buffer, pH 6.5, and 10% D_2O for field/frequency lock. Standard ^{1}H, ^{15}N FHSQC experiments were recorded at 298 K with a Bruker Avance 800 MHz NMR spectrometer equipped with a cryogenically cooled probe. Ligands were dissolved in deuterated acetonitrile to a concentration of 23 mM. For each ligand, HSQC experiments were recorded with protein:ligand ratios of 1:5, 1:10, and 1:20. A set of reference experiments was recorded by adding the same amount of deuterated acetonitrile without any ligand to the protein solution.

Normalized chemical changes were expressed as weighted geometric average of chemical shift changes (^{1}H and ^{15}N) by normshift = $(\delta(^1H)^2 + (0.1\delta(^{15}N))^2)^{1/2}$. Normalized chemical shift changes larger than 0.03 ppm were considered as significant.

Infection Assay of U937 Cells. The human macrophage-like cell line U937 was infected as described previously.[20] In brief, cells were infected with a multiplicity of infection (MOI) of 10 with or without 50 μM of substance **B** (***S*-4c**) or rapamycin. The used bacterial strains were *L. pneumophila* Philadelphia-1 JR32 (wild type, WT), the MIP-negative mutant *L. pneumophila* Philadelphia-1 JR32−2[3], and the *E. coli* strain HB101. Two hours after infection, extracellular bacteria were killed by gentamicin and infection samples were plated on BCYE agar to determine CFU counts immediately and after 24 and 48 h. During incubation of the respective samples, 50 μM of rapamycin or substance **B** (***S*-4c**) were always present. Control experiments showed that rapamycin and substance **B** (***S*-4c**) do not alter replication rates of bacterial cultures.

Acknowledgment. Financial support by the Deutsche Forschungsgemeinschaft (SFB 630) is gratefully acknowledged.

Supporting Information Available: Experimental details of the synthesis, analytical and spectral data of all synthesized compounds. This material is available free of charge via Internet at http://pubs.acs.org.

References

(1) Steinert, M.; Hentschel, U.; Hacker, J. *Legionella pneumophila:* an aquatic microbe goes astray. *FEMS Microbiol. Rev.* **2002**, *26* (2), 149–162.
(2) Cianciotto, N. P.; Stamos, J. V.; Kamp, D. W. Infectivity of *Legionella pneumophila* MIP mutant for alveolar epithelial cells. *Curr. Microbiol.* **1995**, *30* (4), 247–250.
(3) Wintermeyer, E.; Ludwig, B.; Steinert, M.; Schmidt, B.; Fischer, G.; Hacker, J. Influence of site specifically altered MIP proteins on intracellular survival of *Legionella pneumophila* in eucaryotic cells. *Infect. Immun.* **1995**, *63* (12), 4576–4583.
(4) Wagner, C.; Khan, S. A.; Kamphausen, T.; Schmausser, B.; Unal, C.; Lorenz, U.; Fischer, G.; Hacker, J.; Steinert, M. Collagen binding protein MIP enables *Legionella pneumophila* to transmigrate through a barrier of NCI-H292 lung epithelial cells and extracellular matrix. *Cell. Microbiol.* **2007**, *9*, 450–462.
(5) Gelse, K.; Pöschl, E.; Aigner, T. Collagens—structure, function and biosynthesis. *Adv. Drug Delivery Rev.* **2003**, *12*, 1531–1546.
(6) Fischer, G.; Bang, H.; Ludwig, B.; Mann, K.; Hacker, J. MIP protein of *Legionella pneumophila* exhibits peptidyl-prolyl-*cis*/*trans* isomerase (PPIase) activity. *Mol. Microbiol.* **1992**, *6* (10), 1375–1383.
(7) Ceymann, A.; Horstmann, M.; Ehses, P.; Schweimer, K.; Paschke, A.; Steinert, M.; Faber, C. Solution structure of the *Legionella pneumophila* MIP−rapamycin complex. *BMC Struct. Biol.* **2008**, *8*, 17.
(8) Riboldi-Tunnicliffe, A.; König, B.; Jessen, S.; Weiss, M. S.; Rahfeld, J.; Hacker, J.; Fischer, G.; Hilgenfeld, R. Crystal structure of MIP, a prolylisomerase from *Legionella pneumophila*. *Nature Struct. Biol.* **2001**, *8*, 779–783.
(9) Holt, D. A.; Luengo, J. I.; Yamashita, D. S.; Oh, H.; Konialian, A. L.; Yen, H.; Rozamus, L. W.; Brandt, M.; Bossard, M. J.; Levy, M. A.; Eggleston, D. S.; Liang, J.; Schultz, L. W.; Stout, T. J.; Clardy, J. Design, Synthesis, and Kinetic Evaluation of High-Affinity FKBP Ligands and the X-ray Crystal Structures of Their Complexes with FKBP12. *J. Am. Chem. Soc.* **1993**, *115*, 9925–9938.
(10) Holt, D. A.; Konialian-Beck, A. L.; Oh, H.; Yen, H.; Rozamus, L. W.; Krog, A. J.; Erhard, K. F.; Ortiz, E.; Levy, M. A.; Brandt, M.; Bossard, M. J.; Luengo, J. Structure−activity studies of synthetic FKBP Ligands as peptidyl-prolyl isomerase inhibitors. *Bioorg. Med. Chem. Lett.* **1994**, *4*, 315–320.
(11) Fischer, G.; Mech, C.; Bang, H. Nachweis einer Enzymkatalyse für die cis/trans Isomerisierung der Peptidbindung in prolinhaltigen Peptiden. *Biomed. Biochim. Acta.* **1984**, *43*, 1101–1111.
(12) Köhler, R.; Fanghänel, J.; König, B.; Lüneberg, E.; Frosch, M.; Rahfeld, J. U.; Hilgenfeld, R.; Fischer, G.; Hacker, J.; Steinert, M. Biochemical and functional analyses of the MIP protein: influence of the N-terminal half and of peptidylprolyl isomerase activity on

the virulence of *Legionella pneumophila*. *Infect*. *Immun*. **2003**, *71* (8), 4389–4397.
(13) Morris, G. M.; Goodsell, D. S.; Halliday, R. S.; Huey, R.; Hart, W. E.; Belew, R. K.; Olson, A. J. Automated docking using a Lamarckian genetic algorithm and an empirical binding free energy function. *J*. *Comput*. *Chem*. **1998**, *19* (14), 1639–1662.
(14) Jones, G.; Willett, P.; Glen, R. C.; Leach, A. R.; Taylor, R. Development and validation of a genetic algorithm for flexible docking. *J*. *Mol*. *Biol*. **1997**, *267* (3), 727–748.
(15) Case, D. A.; Pearlman, D. A.; Caldwell, J. W.; Cheatham, T. E., III; Ross, W. S.; Simmerling, C. L.; Darden, T. A.; Merz, K. M.; Stanton, R. V.; Cheng, A. L.; Vincent, J. J.; Crowley, M.; Tsui, V.; Radmer, R. J.; Duan, Y.; Pitera, J.; Massova, I.; Seibel, G. L.; Singh, U. C.; Weiner, P. K.; Kollman, P. A. *AMBER 6*; University of California: San Francisco, 1999.
(16) Gasteiger, J.; Marsili, M. Iterative partial equilization of orbital electronegativity—a rapid access to atomic charges. *Tetrahedron* **1980**, *36*, 3219–3228.
(17) *SYBYL Molecular Modeling Software*; Tripos Inc.: St. Louis, MO, 2007.
(18) Hamilton, G. S.; Li, J.; Steiner, J. P. Method of using neurotrophic sulfonamide compounds. U.S. Patent US 5721256 A 19980224, 1998.
(19) Bellamy, F. D.; Ou, K. Selective reduction of aromatic nitro compounds with stannous chloride in nonacidic and nonaqueous medium. *Tetrahedron Lett*. **1984**, *25*, 839–842.
(20) Hacker, J.; Ott, M.; Wintermeyer, E.; Ludwig, B.; Fischer, G. Analysis of virulence factors of *Legionella pneumophila*. *Zentralbl Bakteriol*. **1993**, *278* (2−3), 348–358.